Hue University Journal of Science: Natural Science
Vol. 132, No. 1B, 23–32, 2023

pISSN 1859-1388
eISSN 2615-9678

Adsorption capacity of Safranin O dye using chitosan hydrogel beads extracted from *Penaeus monodon* shrimp shell waste

Do Thi My Phuong[1], Nguyen Xuan Loc[2]*

[1] Department of Environmental Engineering, College of the Environment and Natural Resources, Can Tho University, Can Tho 900000, Vietnam
[2] Department of Environmental Science, College of the Environment and Natural Resources, Can Tho University, Can Tho 900000, Vietnam

* Correspondence to Nguyen Xuan Loc <nxloc@ctu.edu.vn>

(*Received: 18 July 2022; Accepted: 01 November 2022*)

Abstract. In this study, chitosan was extracted from *Penaeus monodon* shrimp shell waste and was used as a bio-sorbent to remove Safranin O (SO) dye in aqueous solution. The chitosan adsorbent was characterized by using SEM and FTIR techniques. Batch adsorption experiments were carried out to evaluate the influence of solution pH, chitosan dosage, contact with time, and initial SO concentration on the adsorption process. The study was conducted with varying contact times from 1 to 720 min, adsorbent dose from 0.1 to 3 g, adsorbate concentration from 10 to 200 $mg.L^{-1}$, and pH from 3 to 10. The results showed that adsorption of Safranin O by chitosan reached equilibrium after 120 min and after that a little change of SO removal efficiency was observed. The maximum adsorption capacity of Safranin O calculated by the Langmuir model was 17.86 $mg.g^{-1}$ was obtained at room temperature (25 ±2 °C), pH of 7, chitosan dose 0.2 g, and SO concentration of 50 $mg.L^{-1}$. The kinetics of the adsorption process followed the pseudo-second-order kinetics model with the correlation coefficient R^2 of 0.95. The Langmuir and Freundlich adsorption isotherm models described well the Safranin O adsorption process, with R^2 of higher than 0.95. The study demonstrated that the chitosan can be extracted from *Penaeus monodon* shrimp shells simply and can be effectively used to remove Safranin O cationic dye in aqueous solution.

Keywords: adsorption, chitosan, Safranin O, shrimp shell

1 Introduction

Synthetic dyestuffs are the major water pollutants discharged by the leather, paint, paper, textile, food processing and printing industries [1, 2] which contribute to environmental contamination and serious health problems due to their extensive application [3]. Most of the organic dyes used in various industrial processes are found to be toxic, stable to oxidizing agents, resistant to biodegradation because of their large molecular size and complexity of their structure [4]. They also adversely affect the metabolic functions of microalgae and aquatic plants by interfering with the biological activity of microalgae and aquatic plants [5]. Safranin O (SO), a basic cationic dye, has been extensively used in paper technology as counterstain to cotton blue stain for fungal hyphae. SO dye has a complex organic structure which contribute to its mutagenic, genotoxic and carcinogenic properties in a wide range of living beings, therefore, the presence of SO in natural water bodies could pose risks to the aquatic ecosystem and human health [6]. Thus, investigation of appropriate technologies for the removal of toxic dyes as SO from the wastewater before discharging them into the water bodies is of utmost importance.

During the last few years, several physicochemical methods have been used for the removal of dyes from wastewater effluent, including photo-catalytic degradation [7, 8], coagulation and ultrafiltration [9, 10], electrochemical [11, 12], oxidative degradation [13, 14], adsorption [6, 15], and other electrochemical methods [16, 17]. Among these methods, dye removal by using different bio-sorbents is considered to be more economical and effective method. Natural polysaccharide polymers, such as chitosan, have attracted attention because they are biodegradable, non-toxic and environmentally friendly. Chitosan is an amino polysaccharide, produced from the deacetylation of chitin obtained from crustaceans and insects. Chitosan consists of β-1,4-linked 2-amino-2-deoxy-β-D-glucose (deacetylated D-glucosamine) and N-acetyl-D-glucosamine units. Each D-glucosamine unit contains a free amino ($-NH_2$) group, and these groups can take on a positive charge which make a good chelating ligand capable of binding to metal ions or dye ions. In the literature, extensive research on chitosan hydrogel beads has proven its potential as a cheap and effective adsorbent to remove either heavy metals or anionic dyes from aqueous solution [18, 19]. However, little research was done to explore the potential application of chitosan in removal cationic dyes (such as Safranin O) from aqueous solution.

Therefore, in this study, chitosan extracted from *Penaeus monodon* shrimp shell waste was fabricated as a bio-sorbent for SO removal from aqueous solution. The characteristics of the chitosan were determined by SEM (Scanning Electron Microscopy) and FTIR (Fourier Transform Infrared Spectroscopy). Main affecting factors for the adsorption process were thoroughly investigated in this study, including solution pH (varying from 3 to 10), contact time (varying from 1 to 720 min), adsorbent dose (varying from 0.1 to 3 g) and adsorbate concentration (varying from 10 to 200 $mg.L^{-1}$), by using batch adsorption studies. Also, adsorption isotherms including Langmuir and Freundlich models were used to evaluate the adsorption capacity of the chitosan extracted from *Penaeus monodon* shrimp shell waste against SO ions. Whereas pseudo–first-order and pseudo-second-order kinetic models were analyzed to define the adsorption kinetics of SO ions in aqueous solution.

2 Materials and Methods

2.1 Chemicals

All chemicals used in this study included acetic acid CH_3COOH, hydrochloric acid HCl, sodium hydroxide NaOH (China), and Safranin O (Sigma-Aldrich).

2.2 Chitosan extraction process

Raw material *Penaeus monodon* shrimp shell waste was collected from local seafood company in Vietnamese Mekong Delta and used in this study, following the procedure of Radwan et al. [20].

Firstly, shrimp shell waste was washed with tap water several times to remove contaminants. Next, the pink shrimp shells were dried at 60 °C overnight, then were ground to a fine powder before preparation of chitin and chitosan. Further steps were followed the procedure as outlined in Fig. 1. The resulting samples from this step are identified as chitosan and used for SO adsorption experiment.

pISSN 1859-1388
eISSN 2615-9678

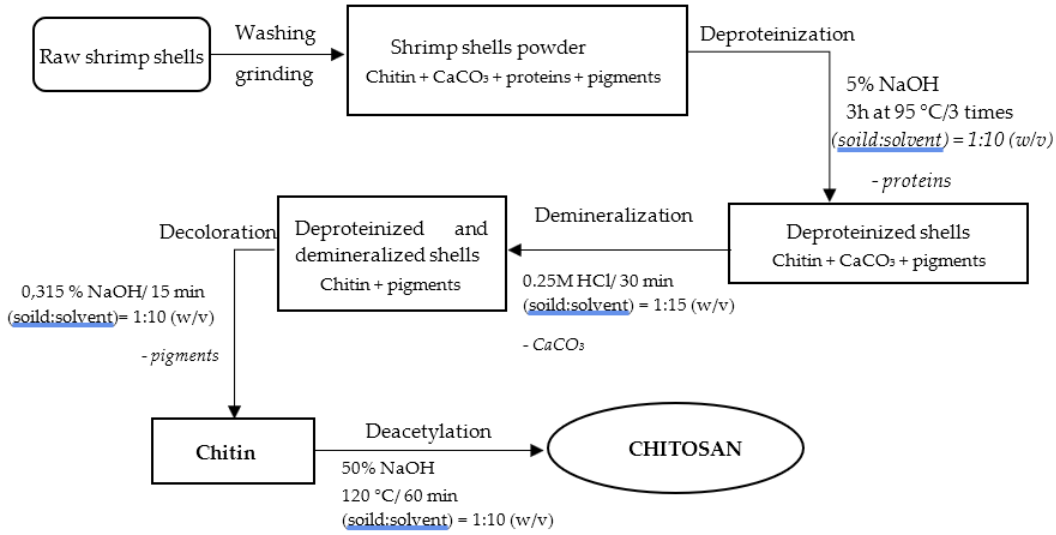

Fig. 1. Chitin and chitosan production flow scheme

2.3 Characterization of chitosan

The micrographs of chitosan were evaluated by scanning electron microscopy (SEM, Hitachi S4800, Japan), while their functional groups were analyzed using a Fourier transform infrared spectroscopy (FTIR, FTIR-PerkinElmer Spectrum 10.5.2).

2.4 Batch Adsorption Experiments

The batch adsorption experiments were used to evaluate the adsorption performance of chitosan against SO in aqueous solution. In a typical experiment, the fixed quantity of chitosan and 10 mL SO solution were added into #15 mL conical centrifuge tubes. The flasks were agitated in a shaker (HS 250 Basic, IKA Labortechnik) at 120 rpm at room condition (25 ± 2 °C) for a fixed time. The solutions were filtered by Whatman No. 1 filter paper (pore size, 11 μm). After filtering, the residual SO in solution was analyzed by measuring the SO at an optimal wavelength of 530 nm (corresponding to the maximum adsorption capacity for SO), using UV-Vis spectroscopy (Shimazdu UV-1900, Japan). To increase the accuracy of the data, each experiment was repeated 3 times.

The SO adsorbed at equilibrium, q_e (mg.g^{-1}) of chitosan and percentage removal (or removal efficiency) of SO dye were determined by the Eq. (1) and Eq. (2), respectively:

$$q_e = \frac{C_0 - C_e}{m} V \quad (1)$$

$$H = \frac{(C_0 - C_e).100}{C_0} \quad (2)$$

where C_0 (mg.L^{-1}) is the initial SO concentrations; C_e (mg.L^{-1}) is the SO concentrations at equilibrium; m (g) is the mass of adsorbent; V (mL) is the volume of the solution.

2.5 Adsorption kinetics

To examine the adsorption mechanisms involved in removal of SO dye by chitosan, pseudo-first-order and pseudo-second-order kinetic models were used to analyze the kinetic experimental data. The pseudo–first-order (PFO) model and pseudo-second-order (PSO) model can be described by the following Eq. (3) and Eq. (4), respectively:

$$q_t = q_e(1-\exp^{-k1t}) \quad (3)$$

$$\frac{dq_t}{dt} = k_2(q_e - q_t)^2 \quad (4)$$

where q_e (mg.g^{-1}) is the equilibrium adsorption capacity; q_t (mg.g^{-1}) is the adsorption capacity at given time t; k_1 (1.min^{-1}) is rate constant of pseudo-first-order adsorption; k_2 (g.mg^{-1}.min^{-1}) is rate constant of pseudo-second-order adsorption.

2.6 Adsorption isotherm

To predict the adsorption behavior of chitosan for SO, Langmuir and Freundlich isotherm models were applied. The nonlinear models for Langmuir and Freundlich isotherm models are shown in Eq. (5) and Eq. (6), respectively:

$$q_e = \frac{q_m K_L C_e}{1+K_L C_e} \quad (5)$$

$$q_e = K_F C_e^{1/n} \quad (6)$$

where q_e (mg.g^{-1}) is the adsorption capacity at equilibrium; q_m (mg.g^{-1}) is theoretical maximum adsorption capacity; C_e (mg.L^{-1}) is the concentration of the adsorbate at equilibrium; K_L (L.mg^{-1}) is the Langmuir adsorption constant; K_F ((mg.kg^{-1})/(mg.L^{-1})^n) is the Freudlich adsorption constant; 1/n is the intensity of adsorption (unitless).

3 Results and Discussion

3.1 Characteristics of chitosan

The scanning electron microscopy (SEM) images (at magnification of ×500 and scale bar of 100 μm) of chitosan extracted from *Penaeus monodon* shrimp shells is shown in Fig. 2. It is observed that chitosan exhibited a nonporous surface and smooth membranous phase.

The infrared spectrum of chitosan is shown in Fig. 3. The absorption bands at around 3784 cm^{-1} and 2874 cm^{-1} can be attributed to O-H stretching and C-H asymmetric stretching, respectively. The presence of residual N-acetyl groups was confirmed by the bands at around 1648 cm^{-1} (C=O stretching of amide I) and 1316 cm^{-1} (C-N stretching of amide III), respectively. The CH_3 symmetrical deformations were

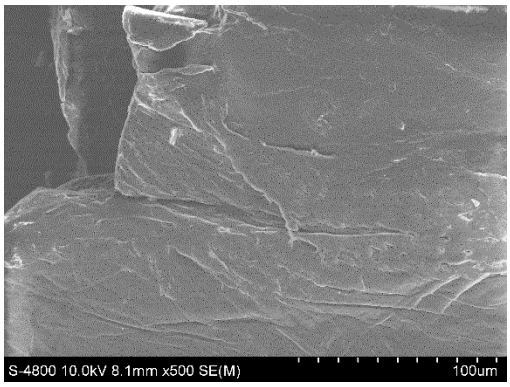

Fig. 2. SEM images of chitosan

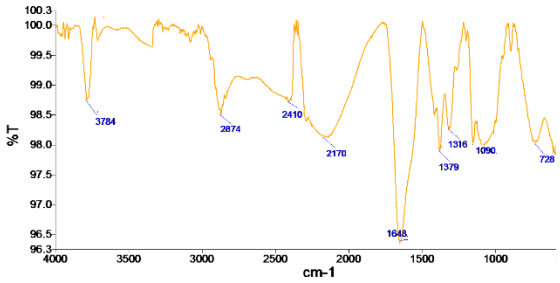

Fig. 3. FTIR spectra of the chitosan

confirmed by the presence of bands at around 1379 cm^{-1}. The absorption band at 1090 cm^{-1} can be attributed to the free amino group (−NH_2) at glucosamine C_2 position. Chitosan FTIR spectra also showed bands at 573 cm^{-1} and 728 cm^{-1} corresponds to C–O stretching and N-H stretching, respectively. All bands are found in the spectra of samples of chitosan reported by others [20, 21].

3.2 Effects of solution pH

The solution pH plays an important role in the entire adsorption process, since it affects the surface charge of the adsorbent. The effect of the solution pH on the adsorption capacity of SO by chitosan were performed in the range of 3 –10 at room temperature (25 ±2 °C). Fig. 4 shows that the removal efficiency of SO adsorption to chitosan were highly pH-dependent. The removal efficiency increased rapidly when increasing the pH from 3 to 7 (increased from 14.45 to 48.46 %),

pISSN 1859-1388
eISSN 2615-9678

continuously increasing pH solution from 7 to 10, the removal efficiency still increased, however, the increasing values were slowed down and almost insignificant (from 48.46 to 55.93 %, increased by approximatedly 7%). To explain, at pH below 6, the amino groups (–NH_2) of the chitosan are protonated to form cationic amino group (–NH_3^+), leading to a decrease in electrostatic repulsion between adsorbate-adsorbent interactions, as indicated by the drop in removal efficiency at acidic environment [23]. On the contrary, in alkaline environment, a decrease in the positive charge of the amine groups (-NH_2) of chitosan can occur due to an excess of -OH molecules, hence the surface charge of the chitosan becomes more negative, resulting a strong adsorbate-adsorbent interactions (by electrostatic attraction), thereafter increasing the removal efficiency [23].

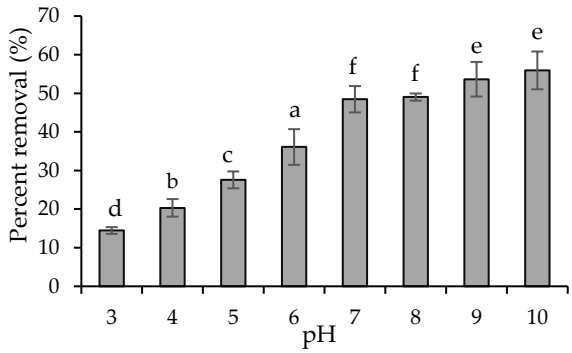

Fig. 4. Effect of pH on the removal efficiency of SO

Note: Data expressed as mean ± SD. Values with different alphabets (a, b, c, …g) were significance ($p < 0.05$).

In summary, the removal efficiency of SO at pH ~ 7 was more appropriate than the remaining pH values, so pH ~ 7 was selected for further adsorption experiment.

3.3 Effect of chitosan dosage

The adsorbent dosage is also one of the essential factors to the adsorption process, where the removal efficiency increases in proportion to the amount of adsorbent added until a specified point is reached [24]. Fig. 5 shows that the percent SO removal increased from 33.97 to 59.41 % with increasing chitosan dosage from 0.1 to 3.0 g. In other words, the SO percent removal was proportional to the chitosan dosage, that is, increasing the chitosan dosage led to a rise in the percent removal of SO. It can be explained that by the increase in the chitosan dosage, the number of active sites increases and thus removal percentage increases. However, when the active sites on the chitosan surface reach saturation, any increase in chitosan dosage will not significantly change the adsorption capacity, as found in this study. These trends were similar to other studies of using chitosan for the removal of dye in aqueous solution [25, 26].

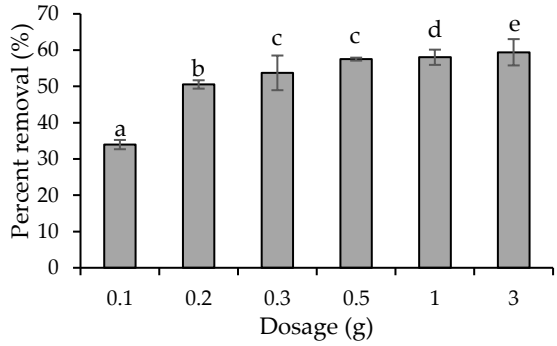

Fig. 5. Effect of chitosan dosage on the percent removal of SO

Note: Data expressed as mean ± SD. Values with different alphabets (a, b, c, …g) were significance ($p < 0.05$).

In this study, the dosage of 0.2 g chitosan was selected for the following experiments.

3.4 Effect of contact time

Contact time is another important parameter that should be investigated in adsorption because it can reflect the adsorption kinetics of an adsorbent for a given concentration of the adsorbate [27]. In this experiment, all of the parameters except contact time, including temperature (25 ±2 °C), chitosan dosage (0.2 g), pH (7), initial SO concentration (50 $mg.L^{-1}$) were kept constant. The

effect of contact time on SO removal efficiency showed in Fig. 6. It is observed from Fig. 5 that the uptake of SO ion occurred in two stages, with an initial rapid uptake, then followed by subsequent slow uptake. More specifically, the adsorption process appeared to proceed rapidly in the first 120 min with the percent removal increased from 21.21 to 67.43 %, and afterwards no significant change was observed (increased by 8%). To explain, as time of adsorption was changed from 1 to 120 min, the numbers of available active sites were much larger than the number of SO molecules to be adsorbed, resulting a highly efficient removal of SO in aqueous solution by the chitosan. There was no significant change in equilibrium concentration after 120 min, the adsorption process reached to equilibrium. Such behavior is in agreement with that observed in other studies [27, 28].

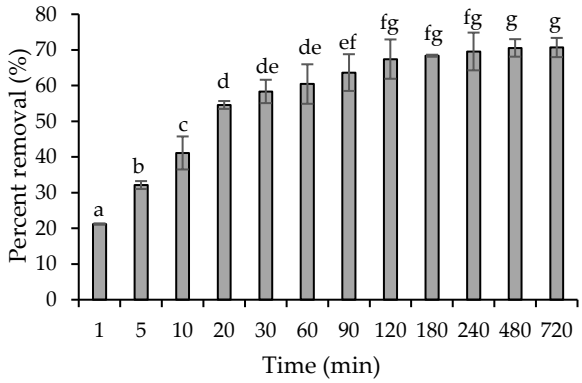

Fig. 6. Effect of contact time on the percent removal of SO

Note: Data expressed as mean ± SD. Values with different alphabets (a, b, c, …g) were significance ($p < 0.05$).

Therefore, the contact time of 120 min was chosen for all experiments.

3.5 Effect of initial SO concentration

Initial adsorbate concentration is also one of the significant factors affecting the adsorption efficiency of an adsorbent. The experiments of the effect of initial SO concentration on removal efficiency were done with variable initial SO concentration (10, 30, 50, 80, 100, 120, 150, 180 and 200 $mg.L^{-1}$) and constant temperature (25 ±2 °C), pH (7), contact time (120 min) and chitosan dose (0.2 g). The experimental results were presented in Fig. 7. As Fig. 7 is shown, SO removal efficiency decreased with the increase in initial SO concentration. To be more specific, the removal efficiency decreased from 76.43 (at C_e = 10 $mg.L^{-1}$) to 29.82 % (at C_e = 200 $mg.L^{-1}$). To explain, at low SO concentrations of 10 – 50 $mg.L^{-1}$, the ratio of the initial number of moles of SO ions to the available surface area of chitosan is large and subsequently the fractional adsorption becomes independent of initial SO concentration, so the percentage removal is high (> 60 %). However, at higher concentrations (C_e > 50 $mg.L^{-1}$), the available sites of adsorption become fewer, while number of moles of SO ions increases, hence the percentage removal of SO ions depends upon the initial concentration, decreases the percentage removal. Such trend is in agreement with that observed in other studies [28].

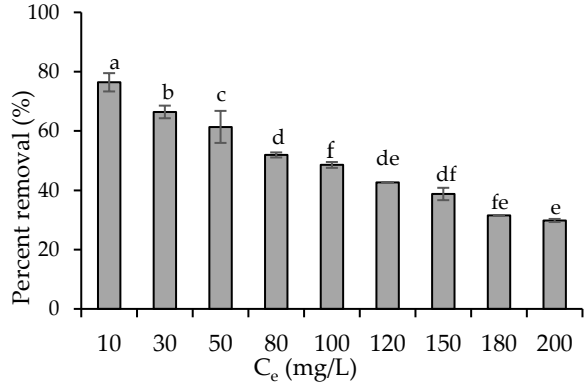

Fig. 7. Effect of SO concentration on the removal efficiency

Note: Data expressed as mean ± SD. Values with different alphabets (a, b, c, …g) were significance ($p < 0.05$).

pISSN 1859-1388
eISSN 2615-9678

In this experiment, initial SO concentration of 50 mg.L^{-1} was chosen as the suitable concentration for SO adsorption of chitosan.

3.6 Adsorption kinetics

In order to define the adsorption kinetics of SO ions, the adsorption kinetic models for the adsorption process were studied for contact times ranging from 1 to 720 min. The kinetic experimental data at constant temperature (25 ±2 °C), dosage (0.2 g), pH (7), initial SO concentration (50 mg.L^{-1}). The non-linear fits of pseudo-first-order (PFO) and pseudo-second-order (PSO) kinetic models are displayed in Fig. 8. All the calculated kinetic parameters are presented in Table 1.

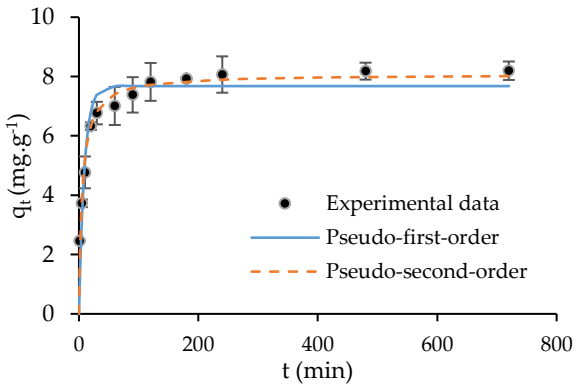

Fig. 8. Plots of PFO and PSO kinetic models for SO adsorption

Table 1. Adsorption kinetic parameters for SO removal

Parameter	PFO	PSO
R^2	0.87	0.95
$q_{e,\,exp}$ (mg.g^{-1})	7.82	7.82
$q_{e,\,cal}$ (mg.g^{-1})	7.68	8.07
k_1 (1.min^{-1})	0.11	-
k_2 (g.mg^{-1}.min^{-1})	-	0.02

It can be confirmed from Table 1 that the pseudo-second order kinetic model was the well-fitted model with comparatively high correlation coefficient (R^2 = 0.95) than the pseudo-first-order model (R^2 = 0.87). The closer values of $q_{e,\,cal}$ (mg.g^{-1}) to $q_{e,\,exp}$ (mg.g^{-1}) in the pseudo-second-order model also demonstrated the fitted better to the experimental data. The fit of the pseudo-second-order model indicated that the rate of adsorption of SO dye onto chitosan was almost a controlled chemisorption process, which involved sharing of electrons between SO dye molecules and surface of chitosan. The adsorption kinetic fitted to the pseudo-second-order kinetic model was also obtained from other chitosan polymers for Congo red dye [29] and Eriochrome black T [30].

3.7 Adsorption isotherms

To obtain the valuable information about the distribution of SO cations on the surface of the chitosan particles, the adsorption isotherms were applied on equilibrium experimental data. The isotherm experimental data performed at various initial SO concentration (10 - 200 mg.L^{-1}), while constant temperature (25 ±2 °C), dosage (0.2 g), pH (7), contact time (120 min) were kept constant. The non-linear fits of Langmuir and Freundlich isotherm models are displayed in Fig. 9. The results showed that both Langmuir and Freundlich adsorption isotherms (Fig. 9) were well suited to the data on equilibrium sorption of SO dye onto chitosan.

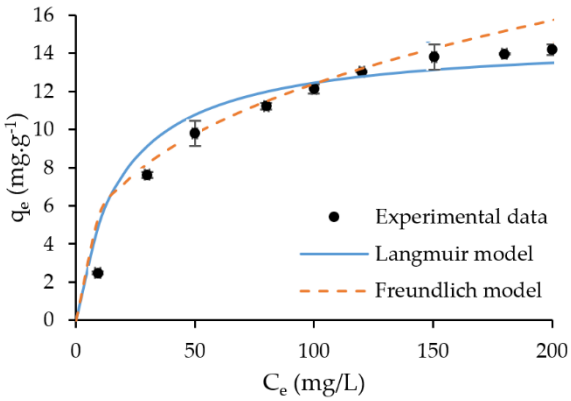

Fig. 9. Plots of Langmuir and Freundlich adsorption isotherms for SO dye adsorption

The outcome values of isotherm parameters for the removal of SO by chitosan are presented in Table 2.

Table 2. Adsorption isotherm parameters for SO removal

Parameter	Langmuir	Freundlich
R^2	0.99	0,.95
q_{max} (mg.g^{-1})	17.86	-
K_L (L.mg^{-1})	0.04	-
K_F (mg.g^{-1})/(mg.L^{-1})^n	-	2.45
1/n	-	2.63

The R^2 values shown in Table 2 indicated a good fit to Langmuir isotherm (R^2 = 0.99) as well as Freundlich isotherm (R^2 = 0.95) to SO for equilibrium adsorption, indicating both the monolayer and multilayer adsorption can be used to explain the adsorption process of SO onto chitosan.

According to the Langmuir isotherm model, the maximum adsorption capacity (q_{max}) values of chitosan for Safranin O at room temperature were calculated as 17.86 mg.g^{-1} (Table 2). A direct comparison was made with other chitosan adsorbents in the recent literature, in which q_{max} for Congo red adsorption on chitosan hydrogel beads [31], chitosan [32] and N,O-carboxymethyl-chitosan/montmorillonite nanocomposite [33] was 92.59, 81.23 and 74.24 mg.g^{-1}, respectively; suggesting that the prepared chitosan hydrogel beads in this study was lower adsorption capacities toward Safranin O dye. However, it is true that no safe comparisons can be made here because the experimental conditions and the adsorbates are different.

4 Conclusion

Penaeus monodon shrimp shell wastes are an abundant source in the Mekong Delta that can be utilized for chitosan production. SEM images showed that the chitosan hydrogel beads exhibited non-porous and smooth surface. The result of FTIR studies revealed different functional groups of organic compounds in chitosan. In this study, essential factors including solution pH, dosage of chitosan, contact time and initial SO concentration all affected removal efficiency of Safranin O by chitosan. The results showed that at room temperature (25 ±2 °C), the SO removal efficiency was highly effective in neutral and alkaline the pH conditions, the chitosan dosage of 0.2 g and the initial SO concentration of 50 mg/L. As the contact time increased, the SO removal efficiency also increased correspondingly, and reached equilibrium in 120 min. The kinetics of adsorption was found to better fit to pseudo-second-order model, indicating a chemisorption mechanism controlled the adsorption process. Both the Langmuir and Freundlich isotherm models described well the adsorption process of Safranin O in solution by chitosan hydrogel beads, which is shown at the correlation coefficients R^2 of higher than 0.95, indicating that the adsorption process can be explained in terms of either monolayer adsorption or multilayer adsorption. The q_{max} values of chitosan for SO at room temperature were calculated as 17.86 mg.g^{-1}. In summary, the *Penaeus monodon* bundant shrimp shell waste can be utilized to produce a chitosan bio-polymer, and has the potential application in the removal of the organic dye Safranin O from aqueous solution.

Acknowledgement

The authors gratefully acknowledge Nguyen Thi Anh Thu, Huynh Cam Nhung, Phan Thi Thanh Tuyen and Nguyen Thi Thanh Thao, for their assistance with the experiment.

References

1. Mittal A, Mittal J, Malviya A, Kaur D, Gupta VK. Adsorption of hazardous crystal violet from

pISSN 1859-1388
eISSN 2615-9678

wastewater by waste materials. Journal of Colloid and Interface Science. 2010; 343:463.

2. Chakraborty S, Chowdhury S, Saha PD. Adsorption of crystal violet from aqueous solution onto NaOH-modified rice husk. Carbohydrate Polymers. 2011;86:1533.
3. Forgacsa E, Cserhatia T, Oros G. Removal of synthetic dyes from wastewaters: a review. Environment International. 2004;30:953.
4. Zhang J, Li Y, Zhang C, Jing Y. Adsorption of malachite green from aqueous solution onto carbon prepared from Arundodonax root. Journal of Hazardous Materials. 2008;150:774.
5. Azari A, Noorisepehr M, Dehganifard E, Karimyan K, Hashemi SY, Kalhori EM, et al. Experimental Design, Modeling and Mechanism of Cationic Dyes Biosorption on to Magnetic Chitosan-Glutaraldehyde Composite. International Journal of Biological Macromolecules. 2019;131:633-645.
6. Phuong DTM, Loc NX. Rice Straw Biochar and Magnetic Rice Straw Biochar for Safranin O Adsorption from Aqueous Solution. Water. 2022; 14(2):186.
7. Zhao DL, Xin Y, Chen CL, Wang XK. Enhanced photo-catalytic degradation of methylene blue on multiwalled carbon nanotubes–tiO2. Journal of Colloid and Interface Science. 2013;398:234.
8. Rajkumar A, Sivarajasekar N, Kandasamy S. Bio-Synthesized Silver Nanoparticles for Effective Photo-catalytic Degradation of Congo Red Dye in Aqueous Solutions: Optimization Studies Using Response Surface Methodology. Analytical Chemistry Letters. 2021;11(6):801-815.
9. Lee JW, Choi SP, Thiruvenkatachari R, Shim WG, Moon H. Submerged microfiltration membrane coupled with alum coagulation/powdered activated carbon adsorption for complete decolorization of reactive dyes. Water Research. 2006;40:435.
10. Beluci NDCL, Mateus GAP, Miyashiro CS, Homem NC, Gomes RG, Fagundes-Klen MR, et al. Hybrid treatment of coagulation/flocculation process followed by ultrafiltration in TiO_2-modified membranes to improve the removal of reactive black 5 dye. Science of the Total Environment. 2019;664:222-229.
11. Shen Z, Wang W, Jia J, Ye J, Feng X, Peng A. Degradation of dye solution by an activated carbon fiber electrode electrolysis system. Journal of Hazardous Materials. 2001;84:107.
12. Nidheesh PV, Zhou M, Oturan, MA. An overview on the removal of synthetic dyes from water by electrochemical advanced oxidation processes. Chemosphere. 2018;197:210-227.
13. Zhao GX, Li JX, Ren XM, Hu J, Hu WP, Wang XK. Highly active MnO_2 nanosheet synthesis from graphene oxide templates and their application in efficient oxidative degradation of methylene blue. RSC Advances. 2013;31:12909.
14. Gemeay AH, El-Halwagy ME, Elsherbiny AS, Zaki AB. Amine-rich quartz nanoparticles for Cu (II) chelation and their application as an efficient catalyst for oxidative degradation of Rhodamine B dye. Environmental Science and Pollution Research. 2021;28(22):28289-28306.
15. Febi IF, Nadya IY, Mai A, Amri S. Adsorption Study of Methylene Blue and Methyl Orange Using Green Shell (Perna Viridis). Journal off Sciences and Data Analysis. 2020;1(1):92-97.
16. Fan L, Zhou YW, Yang WS, Chen GH, Yang F L. Electrochemical degradation of amaranth aqueous solution on ACF. Journal of Hazardous Materials. 2006;137:1182.
17. Fan L, Zhou Y, Yang W, Chen G, Yang F. Electrochemical degradation of aqueous solution of amaranth azo dye on ACF under potentiostatic model. Dyes and Pigments. 2008;76:440.
18. Islam S, Bhuiyan MAR, Islam MN. Chitin and Chitosan: Structure, Properties and Applications in Biomedical Engineering. Journal of Polymers and the Environment. 2017;25:854-866.
19. Coura JC, Profeti D, Profeti LPR. Eco-friendly Chitosan/quartzite Composite as Adsorbent for Dye Removal. Materials Chemistry and Physics. 2020; 256:123711.
20. Radwan MA, Farrag SA, Abu-Elamayem MM, Ahmed NS. Extraction, characterization, and nematicidal activity of chitin and chitosan derived from shrimp shell wastes. Biology and Fertility of Soils. 2012;48(4):463-468.
21. Queiroz MF, Teodosio Melo KR, Sabry DA, Sassaki GL, Rocha HAO. Does the use of chitosan contribute to oxalate kidney stone formation?. Marine drugs. 2014;13(1):141-158.
22. Varma R, Vasudevan S. Extraction, characterization, and antimicrobial activity of chitosan from horse mussel modiolus modiolus. ACS omega. 2020;5(32):20224-20230.

23. Fradj AB, Boubakri A, Hafiane A, Hamouda SB. Removal of azoic dyes from aqueous solutions by chitosan enhanced ultrafiltration. Results in Chemistry. 2020;2:100017.

24. Soltani A, Faramarzi M, Mousavi Parsa SA. A review on adsorbent parameters for removal of dye products from industrial wastewater. Water Quality Research Journal. 2021;56(4):181-193.

25. Raiyaan GID, Khalith SBM, Sheriff MA, Arunachalam KD. Bio-adsorption of methylene blue dye using chitosan-extracted from *Fenneropenaeus indicus* shrimp shell waste. Journal of Aquaculture & Marine Biology. 2021;10(4):146-150.

26. Fradj AB, Boubakri A, Hafiane A, Hamouda SB. Removal of azoic dyes from aqueous solutions by chitosan enhanced ultrafiltration. Results in Chemistry. 2020;2:100017.

27. Dehghani MH, Dehghan A, Alidadi H, Dolatabadi M, Mehrabpour M, Converti A. Removal of methylene blue dye from aqueous solutions by a new chitosan/zeolite composite from shrimp waste: Kinetic and equilibrium study. Korean Journal of Chemical Engineering. 2017;34(6):1699-1707.

28. Subramani SE, Thinakaran N. Isotherm, kinetic and thermodynamic studies on the adsorption behaviour of textile dyes onto chitosan. Process Safety and Environmental Protection. 2017;106:1-10.

29. Mohamed NA, Al-Harby NF, Almarshed MS. Enhancement of adsorption of Congo red dye onto novel antimicrobial trimellitic anhydride isothiocyanate-cross-linked chitosan hydrogels. Polymer Bulletin. 2020;77(12):6135-6160.

30. Boudouaia N, Bengharez Z, Jellali S. Preparation and characterization of chitosan extracted from shrimp shells waste and chitosan film: application for Eriochrome black T removal from aqueous solutions. Applied Water Science. 2019;9(4):1-12.

31. Chatterjee S, Chatterjee S, Chatterjee BP, Guha AK. Adsorptive removal of Congo red, a carcinogenic textile dye by chitosan hydrobeads: binding mechanism, equilibrium and kinetics. Colloids and Surfaces A: Physicochemical and Engineering Aspects. 2007;299(1-3):146-152.

32. Wang L, Wang A. Adsorption properties of Congo red from aqueous solution onto N, O-carboxymethyl-chitosan. Bioresource Technology. 2008; 99(5):1403-1408.

33. Liu W, Zhang L, Chen F, Wang H, Wang Q, Liang K. Efficiency and mechanism of adsorption of low-concentration uranium from water by a new chitosan/aluminum sludge composite aerogel. Dalton Transactions. 2020;49(10):3209-3221.